

Synthesis, Characterization, Thermal degradation studies and Antimicrobial Activity of Novel SASF Copolymer

Satendra M. Sontakke^{1,4}, Akshay A. Akare², Jyotsna V. Khobragade³, W. B. Gurnule^{4*}

¹Department of Chemistry, M. G. Arts, Science and Late N. P. Commerce College, Armori, Maharashtra, India.

²Department of Chemistry, Taywade College, Mahadula, Koradi, Nagpur, India

³Department of Chemistry, Guru Nanak College of Science, Ballarpur, India.

^{4*}Department of Chemistry, Kamla Nehru Mahavidyalaya, Nagpur, Maharashtra, India

E-mail: wbgurnule@gmail.com

Abstract: *In the present study, a novel multifunctional copolymer was synthesized via a controlled polycondensation reaction involving sulphanic acid and semicarbazide with formaldehyde. Structural characterization was carried out using Fourier-transform infrared (FT-IR) spectroscopy, UV-Visible spectroscopy, and proton nuclear magnetic resonance, confirming the successful incorporation of all functional groups within the polymer network. Molecular weight parameters, including number-average and weight-average molecular weights, were determined using gel permeation chromatography (GPC). The results indicated a relatively high molecular weight with a low polydispersity index, reflecting its potential suitability for thermally stable polymer systems. X-ray diffraction analysis revealed a semi-crystalline nature, while scanning electron microscopy demonstrated a uniform and well-defined morphology. The thermal degradation behavior of the copolymer was systematically investigated using thermogravimetric analysis. Kinetic parameters, particularly activation energy (E_a), were calculated using curve-fitting methods based on the Freeman–Carroll and Sharp–Wentworth models, yielding closely matching results that indicate significant thermal stability. Overall, the copolymer exhibits excellent thermal resistance, an organized structural framework, and desirable surface characteristics, making it a strong candidate for advanced applications in high-temperature environments and demanding material engineering sectors. Furthermore, the antimicrobial activity of the copolymer was evaluated against selected bacterial strains, and the inhibition efficiency was measured and reported.*

Keywords: Copolymer, Characterization, Thermal studies, Antimicrobial activity.

I. INTRODUCTION

Multifunctional polymers have become essential materials across a wide range of industrial and technological applications owing to their adjustable structural, thermal, and surface characteristics. The development of such polymers through the incorporation of hydroxyquinoline moieties has demonstrated considerable potential in improving thermal stability, morphological integrity, and overall performance under extreme conditions. The thermal degradation behavior of copolymers represents a key factor in determining their suitability for high-temperature and performance-demanding applications. A polymer's stability under thermal stress governs its resistance to decomposition, maintenance of structural integrity, and durability during processing as well as practical use.

A comprehensive understanding of the kinetic and thermodynamic aspects of thermal degradation provides valuable insights into the structural stability and decomposition mechanism of the polymer, thereby aiding in the design of advanced materials with enhanced performance and reliability [6]. robustness, while also facilitating the development of advanced materials for sensing, electronic, and environmental applications. Due to their structural adaptability and



tunable characteristics, copolymers have become a fundamental component of modern materials research, driving substantial progress across a wide spectrum of industrial domains, including electronics, aerospace, biomedical engineering, and environmental technologies. Gurnule and co-workers investigated the thermal behavior of a copolymer synthesized from benzophenone-3, naphthalene diamine, and formaldehyde, providing important insights into its degradation profile [4].

In another study, a copolymer was prepared through bulk polymerization using phenylhydrazine, carboxyresorcinol, and formaldehyde as precursor monomers [5–7]. Owing to their excellent thermal stability, such copolymers and their derived polychelates have become significant contributors to the advancement of high-performance polymeric materials [8]. In a related investigation, Patel and co-researchers developed a terpolymer resin and its corresponding metal-complexed polychelates, noting that the integration of metal ions within the polymer framework notably diminished its overall thermal stability. [9–11].

Rahangdale performed a comprehensive study on the thermal decomposition behavior of a synthesized copolymer, providing valuable understanding of its heat resistance and overall thermal robustness. [12]. In a similar investigation, thermal characterization was conducted on a copolymer derived from substituted nitrobenzothiazole, oxamide with formaldehyde, demonstrating that the developed composite exhibited markedly improved thermal resistance compared to the parent copolymer. This elevated performance was ascribed to the greater formation of carbonaceous residue, as evidenced by thermogravimetric analysis (TGA) results for both materials [13–14]. Additionally, a copolymer synthesized and characterized from 4-hydroxybenzoic acid, adipamide, and formaldehyde exhibited notably high thermal stability [15–18]. They are extensively utilized in adhesives, surface coatings, and photovoltaic applications [19], and junction transistors [20], primarily because of their favorable combination of thermal stability and ease of processing. In addition to these industrial applications, copolymers have been explored in a variety of advanced functional roles, including as catalysts, ion-exchange resins, activation agents, and high-temperature-resistant materials [21– 22]. Their broad applicability makes them promising candidates for further development in emerging technologies.

An antimicrobial polymer is defined as a class of polymers that possess the ability to inhibit or deactivate the growth and accumulation of microorganisms on surfaces. This activity arises from the incorporation of specific functional moieties, such as amphiphilic segments or polycationic groups, either along the polymer backbone or within the side chains. The antimicrobial action of these polymers is generally nonspecific, primarily involving interactions with microbial cell membranes that lead to disruption of cellular integrity and subsequent inhibition of pathogen proliferation [23].

A copolymer exhibiting effective antimicrobial properties was synthesized by Burkanudeenthrough the condensation polymerization of anthranilic acid, urea, and formaldehyde as monomeric precursors. developed and investigated a polymeric resin along with its composite for the selective removal of toxic metal ions from wastewater [24–26].

The synthesis of copolymers capable of incorporating the functional attributes of individual monomers was undertaken in view of the differing properties of the selected starting materials. The resulting copolymer was subjected to detailed characterization using elemental analysis, UV–Visible spectroscopy, Fourier-transform infrared analysis together with proton (¹H) nuclear magnetic resonance techniques, in addition to determining the number-average molecular weight by gel permeation chromatography. whereas thermogravimetric analysis was utilized to determine its heat resistance. Additionally, the decomposition pattern and associated kinetic parameters were extracted from the TGA results to obtain a more comprehensive understanding of the polymer’s decomposition behavior and an antimicrobial activity was examine.

II. EXPERIMENTAL METHODS

Synthesis of SASF Copolymer

The SASF copolymer was synthesized through a polycondensation reaction conducted in 1 M hydrochloric acid medium. The reaction was carried out using a 1:1:2 molar proportion of sulphanic acid, semicarbazide, and formaldehyde. The Blend was refluxed at 120 °C for 5 h, Subsequent in the formation of a Pail yellow, resinous product. The primary cleaning step was accomplished through sequential rinsing with diethyl ether followed by heated distilled water. For



enhanced purification, the unrefined copolymer was solubilized in an 8% (w/v) aqueous sodium hydroxide medium and then slowly precipitated again by the gradual addition of a combined solution of con. HCl and distilled water. As resulting solid mass was subsequently crushed into a uniform fine particulate form and screened through a mesh to ensure consistent granularity. The copolymer demonstrated remarkable dissolution behavior in organic media including DMSO, DMF, and THF, reflecting favorable affinity toward these solvents. In contrast, its poor dissolution in mineral acids implied minimal compatibility within acidic conditions.

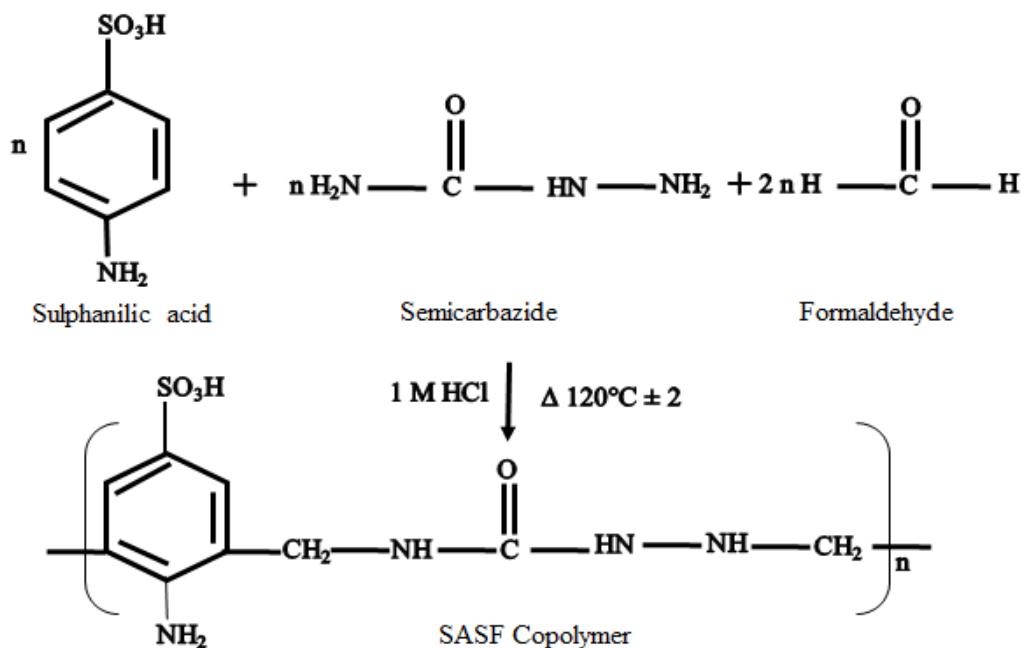


Figure 1: Synthesis of SASF copolymer

III. RESULTS AND DISCUSSION

Elemental Analysis

To establish the composition of the carbon (C), hydrogen (H) and nitrogen (N) composition of the synthesized copolymer resin in percentage. The theoretically calculated values were observed to be in good accord with the experimental values which complicated the successful formation of the copolymer structure. Nitrogen in the polymer structure validates the presence of acryamide units into the polymer backbone with the oxygen-based functional groups being formed by condensing 2, 4-dihydroxybenzoic acid and formaldehyde. Elemental analysis thus presents good support to the successful production of the copolymer resin [27].

Table 1: Elemental analysis and empirical formula of SASF copolymer

Copolymer	% of C Observed (Cal.)	% of H Observed (Cal.)	%N Observed (Cal.)	%S Observed (Cal.)	Empirical Formula of Repeated Unit	Empirical Formula Weight
SASF	41.22 (39.70)	4.59 (4.41)	11.83 (12.04)	2.52 (3.09)	C ₉ H ₁₂ N ₄ SO ₄	272



Molecular Weight Determination by Gel Permeation Chromatography (GPC)

Gel permeation chromatography (GPC) was used to calculate the molecular weight distribution of the produced copolymer. The analysis of the GPC revealed the determination of number average molecular weight (M_n), weight average molecular weight (M_w) and polydispersity index (PDI) of the synthesized copolymer. The GPC analysis revealed that the synthesized copolymer has an intermediate distribution of molecular weight, which is typical of condensation polymerization reactions. Polydispersity index (PDI) gives data concerning uniformity of the polymer chains. A smaller PDI goes to show the evenness of the polymer chains as the polymerization process takes place [28].

Table 2: Molecular Weight Determination of SASF Copolymer by Gel Permeation Chromatography (GPC)

Polymer	Mass of Empirical Unit (g)	Number-Average Molecular Weight (M_n)
SASF	312	3235

UV-Visible Spectroscopy

The electronic transitions of the synthesized copolymer were studied by UV-Visible spectroscopy. The UV-Visible spectrum of the copolymer had absorption bands at the region of 245-265 nm and 368-377 nm which can be attributed to $\pi \rightarrow \pi^*$ and $n \rightarrow \pi^*$ rings and carbonyl groups in the structure of the polymer. The peaks of the absorption in the UV spectrum verify the existence of conjugated aromatic systems and functional groups in the copolymer matrix. These functional groups are responsible for interaction with metal ions during ion-exchange processes [29].

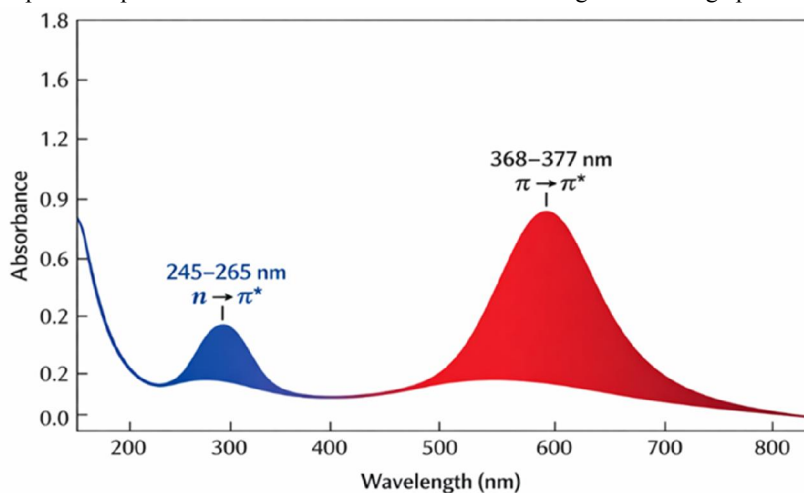


Fig. 2. Ultraviolet-Visible Absorption Spectrum of SASF Copolymer

Fourier Transform Infrared spectroscopy

The broad bond at 3470 cm^{-1} may be attributed to stretching vibration of amino group ($-\text{NH}_2$) within polymer chain. Characteristic stretching vibration in the range of 2916 cm^{-1} may cause due to Aryl C-H stretching frequency. A sharp peak at 1600.70 cm^{-1} indicates $-\text{C}=\text{O}$ stretching vibration of carbonyl group which is the part of semicarbazide moiety [30]. The characteristic peak at 1494 cm^{-1} corresponds to CH_2 bending and wagging vibrations. A sharp and intense band at 1030.84 cm^{-1} indicates the presence of $\text{S}=\text{O}$ symmetric stretching vibration frequencies, whereas the bands at 1165 cm^{-1} are attributed to its asymmetric stretching. The FTIR spectrum of SASF copolymer is depicted in figure 3 and its spectral information was organized in table 3.



Table 3: Fourier Transform Infrared spectral analysis of SASF copolymer

Observed frequencies (cm ⁻¹)	Assigning groups	Expected frequencies (cm ⁻¹)
3470 (b, s)	N-H stretching for amino group	3500-3200
2916 (m)	Aryl-C-H stretching frequency	2900-2500
1600.70 (m)	C=O stretching of semicarbazidemoiety	1600-1500
1494.36	-CH ₂ bending and wagging	1500-1300
1030.84	S=O symmetric stretching	1080-1030
1165	S=O Asymmetric stretching	1230-1160

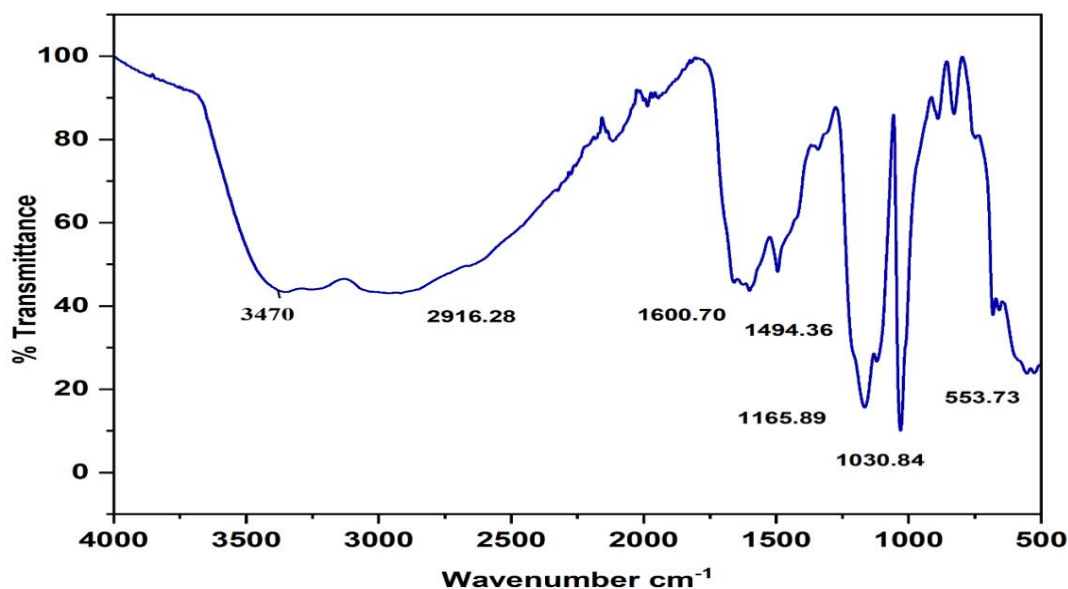


Figure 3: Fourier Transform Infrared spectra of SASF copolymer

¹H NMR Study of Synthesized Copolymer

The spectral data (Figure 5) were interpreted with reference to reported literature. A distinct sharp peak observed at δ 2.67 ppm is recognized to the methylene (-CH₂-) protons. The signals appearing in the region of δ 6.68–7.63 ppm correspond to the aromatic protons of the benzene ring. A weak singlet at δ 9.5 ppm confirms the presence of the -SO₃H functional group. Additionally, a sharp signal at δ 5.36 ppm is assigned to the Ar-CH₂-NH moiety, supporting the proposed structure of the copolymer[31].

Table 4: ¹H NMR analysis for SASF copolymer

Observed chemical shift value in SAMF	Type of proton assigning	Accepted range for chemical shift (δ)ppm
2.67	Ar-CH ₂ moiety	2.0-3.0
5.36	Ar-CH ₂ -N	5.10-7.00
6.68-7.63	Ar-H aromatic ring proton	6.5-8.5
9.5	Proton of acidic linkage SO ₃ H group	8.00-10.00



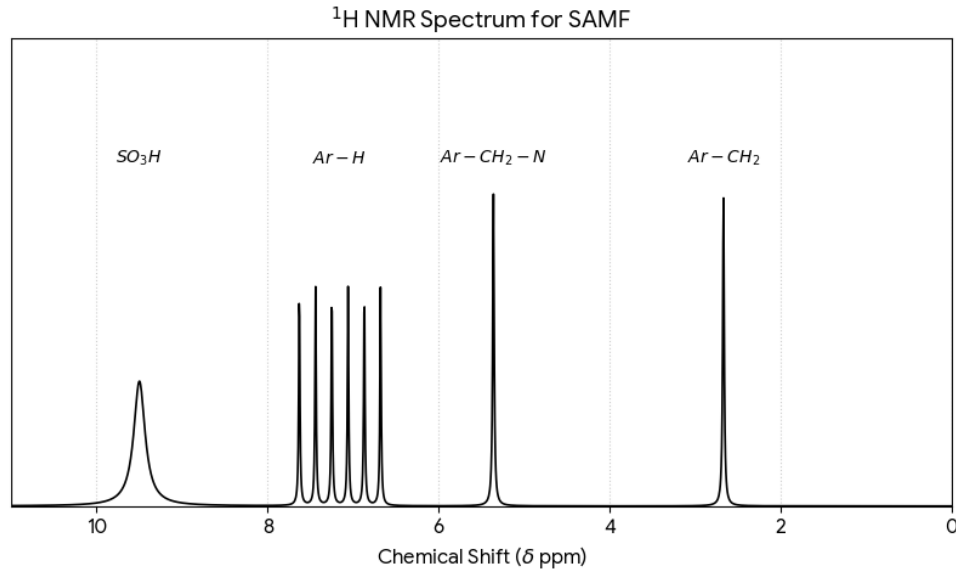


Figure 3: ¹H NMR graph for SASF copolymer

X-ray diffraction

The XRD profile of the synthesized SASF copolymer reveals both amorphous and crystalline characteristics. Broad humps in the diffraction pattern indicate amorphous regions, whereas sharp, intense peaks confirm the presence of crystalline domains. This combination of features demonstrates that the copolymer exhibits a semi-crystalline nature with mixed structural organization [32]. Figure 3 XRD graph shows both features high intensity with narrow band and small broadness. However, the presence of a broad characteristic peak is indicative of significant amorphous content, implying that the copolymer possesses a semi-crystalline nature with both ordered and disordered structural regions.

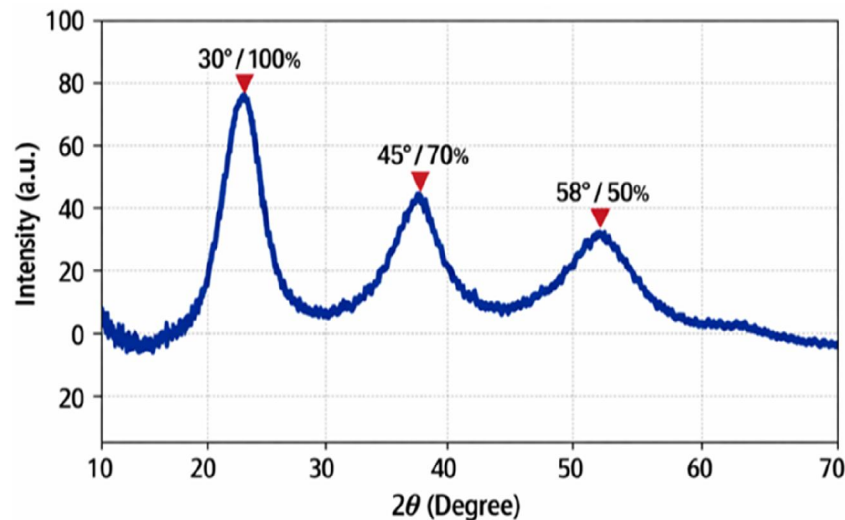


Figure 4: X-ray diffraction (XRD) outline of SASF copolymer



Scanning Electron Microscopy (SEM)

Morphology of synthesized copolymer was studied by Scanning Electron Microscopy. Figure 4 shows the SEM images of the SASF copolymer at $\times 500$, $\times 1000$, $\times 3000$, and $\times 6000$ magnifications. Microstructural analysis reveals spherulitic and fringed features, with a heterogeneous and scattered surface morphology indicative of crystalline–amorphous coexistence [33]. SEM images show dispersed surface regions with fine pits, representing phase transitions between ordered and disordered domains. The presence of fringes supports a semi-crystalline structure, marking interfacial boundaries between crystalline and amorphous phases. The copolymer is thus predominantly amorphous with localized compact regions and deep surface pits.

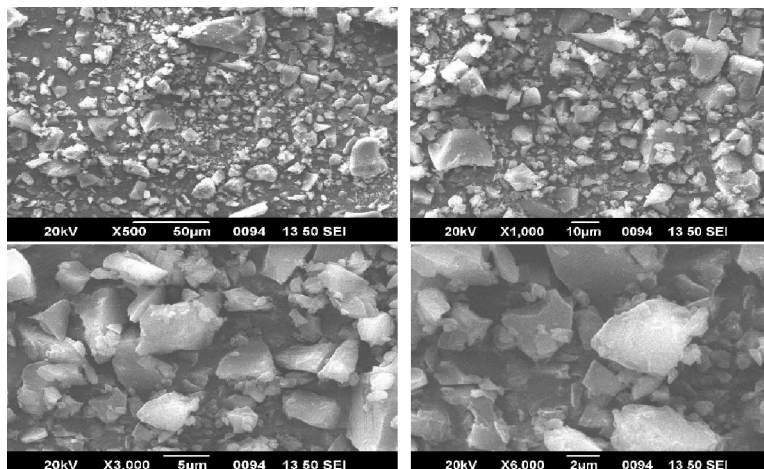


Figure 5: SEM images of magnification at 50µm, 10µm, 5µm and 2µm

Thermo-analytical study of synthesized copolymer

The thermal behavior of the SASF copolymer was evaluated using thermogravimetric analysis (TGA), with the corresponding thermogram shown in Figure 7. The decomposition profile exhibited a characteristic multi-step degradation pattern. In the initial temperature range of 40–160 °C, a minor weight loss of ~2.01% (experimental) and 2.08% (theoretical) was observed, corresponding to the evaporation of physically adsorbed and crystallization-bound water molecules trapped within the polymer matrix [34]. Subsequent thermal decomposition proceeded through three major steps. The first stage, occurring between 160–290 °C, corresponded to the breakdown of phenolic –OH groups linked to the quinoline units, resulting in a weight loss of 37.12% (experimental) versus 36.98% (calculated). This stage reflects the onset of backbone destabilization, cross-linking, and internal stress relaxation leading to partial fragmentation. The second stage, between 290–520 °C, was marked by a sharp weight loss of 82.95% (experimental) and 83.00% (calculated), [35] attributable to decomposition of the –SO₃H group and quinoline aromatic rings, likely through depolymerization, unzipping of cross-linked domains, and thermally induced molecular strain. In the final stage (520–800 °C), further weight loss was recorded due to intensified cross-linking and thermal stress, culminating in near-complete degradation of the polymeric framework. This phase accounted for an almost total mass loss of 99.68% (experimental) compared with 100% (theoretical), leaving negligible residual char. These results highlight the excellent thermal degradation efficiency of the copolymer and confirm its complete disintegration under elevated temperature conditions [36].



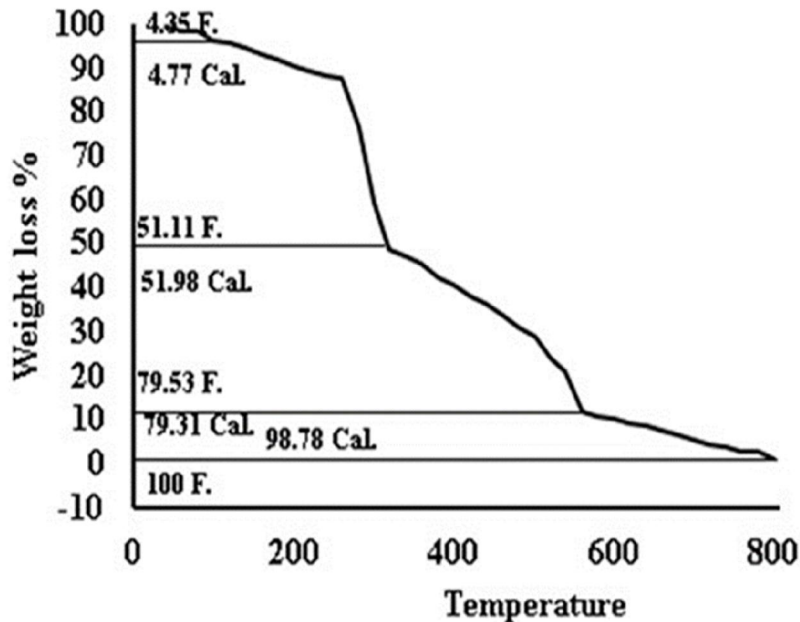


Figure 6. Thermogravimetric curve of SASFCopolymer

Evaluation of Activation Energy Using Sharp–Wentworth Approach

The thermal degradation kinetics of the synthesized polymer were analyzed using the Sharp–Wentworth (SW) method, which provides a reliable means of evaluating activation energy (E_a) from thermogravimetric data. This approach involves linearization of the degradation process to extract kinetic parameters with precision [37]. The activation energy was calculated using the following relationship:

$$\text{Log} \left[\frac{\frac{dc}{dt}}{1-c} \right] = \log \left(\frac{A}{\beta} \right) - \frac{E_a}{2.30 \cdot 3R} \cdot \frac{1}{T} \text{----- (11)}$$

Where:

$\frac{dc}{dt}$ = Change in Weight Loss Fraction as a Function of Temperature

C = Degradation extent at time t

B = Linear heating rate

R = Gas constant

T = temperature

A = Frequency factor

E_a = Activation energy (kJ/mol)

A plot of

$$\text{Log} \left(\frac{\frac{dc}{dt}}{1-c} \right) / \frac{1}{T} \text{----- (12)}$$

Generate a **straight line** to evaluated the activation energy from the **slope**

$$\text{Slope} = \frac{-E_a}{2.30 \cdot 3R} \text{----- (13)}$$

This graphical representation (Figure 7) provides a reliable estimation of the activation energy governing the thermal degradation process, thereby offering valuable insights into the kinetic behavior and thermal stability of the copolymer.



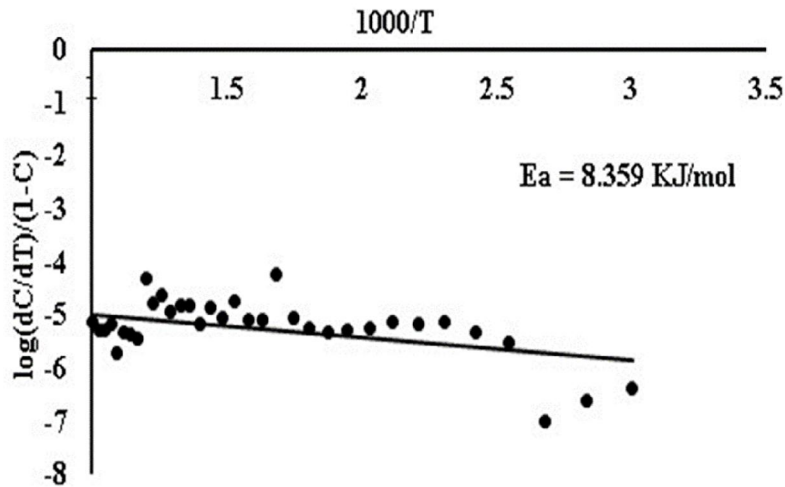


Figure 7. Graphical Determination of Activation Energy via SW Method for SASF Copolymer

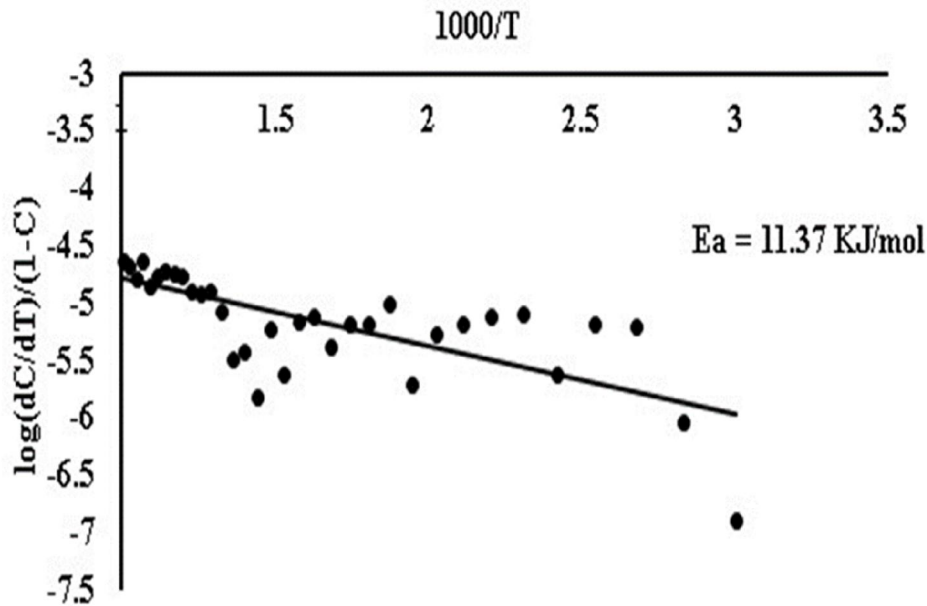


Figure 8. Sharp-Wentworth graph of SASFCopolymer

Kinetic Evaluation Using the Freeman–Carroll Method

To further investigate the thermal decomposition behavior of the polymer, the Freeman–Carroll (FC) method was employed to determine both the activation energy (E_a) and the reaction order (n). This method utilizes a differential approach, directly interpreting thermogravimetric data to extract kinetic parameters [38]. The calculations were performed using the following mathematical expression:



$$\frac{\Delta \log\left(\frac{dw}{dt}\right)}{\Delta \log W_r} = \frac{E_a}{2.30 \cdot 3R} \frac{\Delta\left(\frac{1}{T}\right)}{\Delta \log W_r} + n \text{ ----- (14)}$$

Where:

$\frac{dw}{dt}$ = Mass Accumulation Rate as a Function of Time

$W_r = W_c - W$

W_c = Decreased Mass Observed Upon Completion of the Reaction

W = Decrease in Sample Mass at a Given Time t

E_a = Activation energy (kJ/mol)

R = Gas constant

T = temperature (K)

n = Reaction rate

The activation energy of the polymer resin was determined by evaluating thermogravimetric data through the application of both the Sharp–Wentworth (SW) method (Figure 9) and the Freeman–Carroll (FC) approach (Figure 10). Values obtained from these two independent approaches were found to be closely aligned, reinforcing the reliability and accuracy of the kinetic parameters associated with the polymer’s thermal degradation behavior.

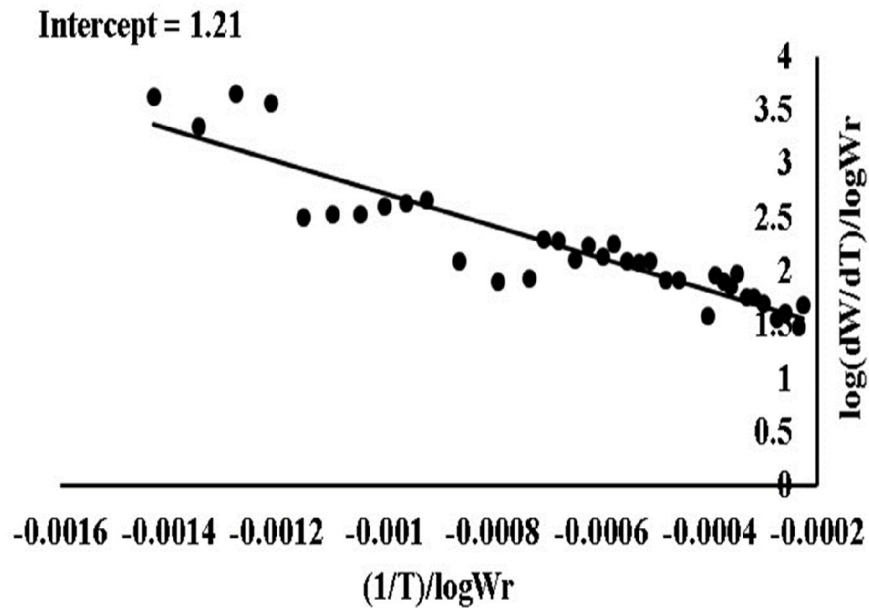


Figure 9. Freeman-Carroll Activation energy graph of SASF Copolymer



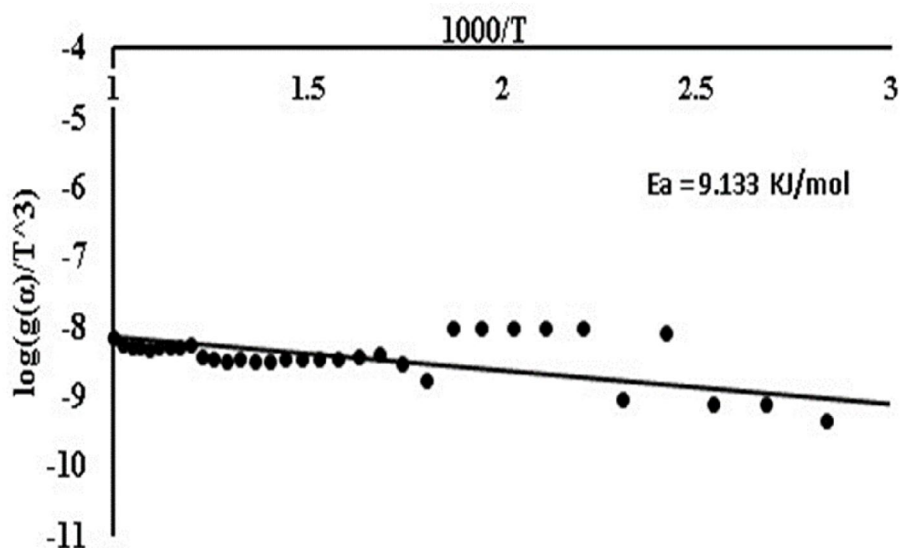


Figure10.Graphical Analysis of Activation Energy and Reaction Order via FC Method

Table 5. Study of Kinetic Profiles and Thermodynamic Variables of the Polymer System

Polymer	Activation KJ mol ⁻¹ (Freeman- Carroll)	Energy[Ea] (Sharp- Wentworth)	Entropy Change (ΔS),(J)	Free energy change(ΔF),KJ	Frequency Factor (Z)Sec ⁻¹	Apparent Entropy change (S*)	Order of reaction (n)
SASF	26.3	28.42	-216.91	113.57	559	-61.33	0.8

The thermal decomposition behavior of the SASFCopolymer was further clarified through the evaluation of key thermodynamic parameters, including Gibbs free energy change (ΔF), entropy change (ΔS), apparent entropy (S), and the frequency factor (Z), as presented in Table 6. The activation energy (E_a) values obtained using both the Freeman–Carroll (FC) and Sharp–Wentworth (SW) methods were found to be in close agreement, demonstrating the reliability and consistency of the kinetic analysis. The relatively low frequency factor (Z) suggests that the degradation proceeds via a comparatively slow mechanism, reflecting the inherent thermal stability and molecular framework of the copolymer. Moreover, the negative entropy change (ΔS) signifies that the transition state is more ordered than the initial state, indicating the formation of a highly structured activated complex during the decomposition process[39-44].

A comprehensive comparison of the activation energy values for each stage of thermal decomposition, calculated using both the Freeman–Carroll and Sharp–Wentworth methods. The consistency between the two datasets reinforces the validity of the applied kinetic models and provides compelling evidence for the inherent thermal stability of the SASF copolymer, confirming its suitability for applications requiring resistance to elevated temperatures.

Antimicrobial Activities of prepared copolymer

Microorganisms, including bacteria, fungi, and parasites, are living entities that serve as major sources of infection. Infectious diseases, caused by pathogenic microbes, account for more deaths worldwide than any other single cause. An antimicrobial is an agent that kills microorganisms or inhibits their growth. Although numerous antimicrobial drugs have been developed for this purpose, many infectious diseases remain challenging to treat. Now a days antimicrobial



polymers, have attracted significant attention in both academic and industrial research. The venerable result was obtained for SASF copolymer against E. coli bacterium which is markedly higher than the standard. E. coli, a gram negative rod-shaped bacterium affects the urinary tracts in humans. Salmonella Typhi abbreviated as S. Typhi is bacteria that spread through contaminated food and water, this bacterium is only found in human and responsible for high fever, headache, stomach ache and weakness. The results showed a good activity against S. aureus, a gram-positive and spherical bacterium leads to life-threatening diseases like pneumonia, osteomyelitis, endocarditis and sepsis. From the experiment, synthesized copolymers were found to have excellent activity against S. aureus species. P. aeruginosa is a common bacterium which can cause diseases like pulmonary tract and urinary tract burns and wounds in animals and human beings.

Table 6. Antimicrobial Activity of SASF copolymer

Copolymer SASF Zone of Inhibition (mm)				
Types	S ₁	S ₂	S ₃	S ₄
S. aureus	19mm	20mm	19mm	20mm
E. coli	16mm	21mm	20mm	15mm
S. typhi	20mm	18mm	19mm	18mm
P. vulgaris	22mm	19mm	21mm	24mm
A. aerogenes	24mm	26mm	25mm	23mm

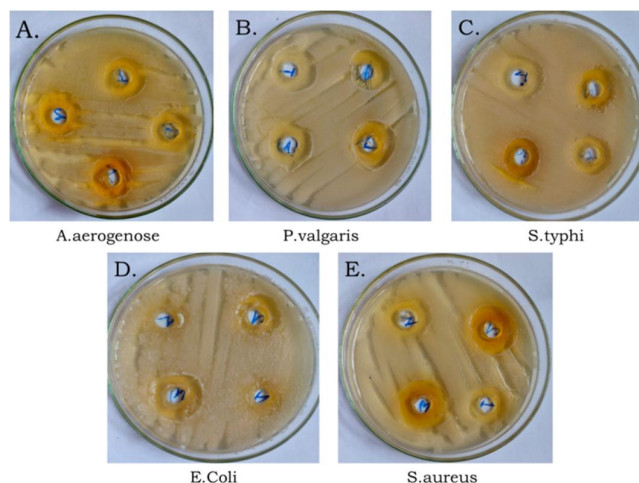


Fig. 11. Antimicrobial Activity of SASF copolymer

IV. CONCLUSION

The SASF copolymer was produced via a polycondensation process, utilizing sulphanilic acid, semicarbazide, and formaldehyde as building blocks, with 1 M HCl serving as the catalyst at a temperature of 120 °C for a duration of 5 hours. Various analytical methods, including elemental testing, FT-IR, ¹H NMR, SEM, and XRD, verified its chemical structure. Thermogravimetric evaluation indicates the material's high heat resistance, as its kinetic variables—such as activation energy, frequency factor, and several entropy and free energy metrics—align closely with the results calculated by the Freeman-Carroll and Sharp-Wentworth techniques. Furthermore, the polymer demonstrates superior antibacterial properties against E. coli, S. aureus, S. typhi, P. vulgaris, and A. aerogenes, a characteristic attributed to the semicarbazide



functional groups within its chain. Consequently, this novel copolymer shows great potential as a next-generation antimicrobial agent.

REFERENCES

1. Gurnule W. B, Das N. C., Vajpai S., Rathod Y. U. Synthesis, characterization and thermal degradation study of copolymer resin. *Mat. Tod. Proc.* 2020; 29: 1071-1076.
2. Gurnule W. B., Juneja H. D., Paliwal L. J. Ion-exchange properties of a salicylic acid–melamine–formaldehyde terpolymer resin. *Rev. & Fun. Polym.* 2002; 50: 95-100.
3. Singru R. N., Zade A. B., Gurnule W. B. Synthesis, characterization, and thermal degradation studies of copolymer resin derived from p-cresol, melamine, and formaldehyde. *J. Appl. Polym. Sci.* 2008; 109: 859-868.
4. Gurnule W. B, Juneja H. D., Paliwal L. J. Ion-exchange properties of salicylic acid–melamine–formaldehyde terpolymer resin. *React. Funct. Polym.* 2002; 50: 95–100.
5. Zade A. B, Singru R. N., Wasudeo B. Gurnule. Thermal degradation and kinetic analysis of phenolic copolymer resins. *J. Appl. Polym. Sci.* 2008; 109: 3315–3320.
6. Gupta R. H, Zade A. B, Gurnule, W. B, Synthesis and characterization of terpolymers derived from 2-hydroxyacetophenone, melamine and formaldehyde. *J. Appl. Polym. Sci.* 2008; 109: 3315–3320.
7. Patle D. B., Gurnule. W. B, Eco-friendly synthesis, characterization and ion-exchange properties of terpolymer resin derived from p-hydroxybenzaldehyde. *Arab. J. Chem.* 2011.
8. Singru R. N., Zade A. B., Gurnule W. B. Synthesis, characterization, and thermal degradation studies of copolymer resin derived from p-cresol, melamine, and formaldehyde. *J. Appl. Polym. Sci.* 2008; 109: 859-868.
9. Gurnule. W. B., Rahangdale S.S. Synthesis and characterization of high-performance terpolymer resin derived from 8-hydroxyquinoline and adipamide. *Der Pharma Chem.* 2011; 3: 235–242.
10. Rahangdale S. S, Das N. C., Vajpai S, Gurnule W. B. Synthesis, Characterization and Thermal degradation studies of Copolymer Resin-II: Resulting from phenylhydrazine, 2, 4-dihydroxybenzoic acid, and formaldehyde. *Int. J. Res. Biosci. Agri. Tech.* 2020; 1: 194-204.
11. Gurnule W. B, Gupta P. G, Gupta R. H, Rathod Y. U, Singru R. N. Thermal degradation studies of 2-amino 6-nitrobenzothiazole-oxamide-formaldehyde copolymer and its composites. *IOP Conf. Ser. Earth Environ. Sci.* 2023; 1281: 012026.
12. Nandekar K. A, Gurnule W. B. SATF-IV copolymer resins: Synthesis, reaction mechanism, structure, and thermodynamic kinetic parameters. *AIP Conf. Proc.* 2024; 3139: 080002.
13. Nandekar K. A., Dontulwar J. N., Gurnule W B. Thermoanalytical studies and kinetics of newly synthesized copolymer derived from p-hydroxybenzoic acid, and semicarbazide. *Rasayan J. Chem.* 2012; 5: 261-268.
14. Rathod Y. U, Pandit V. U, Gurnule W. B. Synthesis, characterization and thermal behavior of 2, 2'-dihydroxybiphenyl-formaldehyde-phenylenediamine copolymer. *Mat. Tod. Proc.* 2022; 53:96-100
15. Rathod Y. U, Gurnule W. B. Synthesis, characterization and thermal behaviour studies of terpolymer resin derived from 8-Hydroxyquinoline-5-sulphonic acid and anthranilic acid. *Current. Appl. Polym. Sci.* 2021; 4: 1-8
16. Akare A.A, Thakre J.N, Khobragade J, Gurnule W. B, Chafle D M. Effective removal of toxic heavy metal ions from aqueous solution using novel selecting copolymer resin. *2026;58(01):952-965.*
17. Rathod Y. U, Zanje S. B, Gurnule W. B. Hydroxyquinoline copolymers synthesis, characterization and thermal degradation studies. *J. Phys.* 2021; 1913: 212061.
18. Rangari M, Rahangdale S.S, Shrivastava S, Rathod Y. U, Waghe P. U, Gurnule W. B. Thermal Degradation Studies of High-Performance Copolymer Resin Derived from 8-Hydroxyquinoline, Acrylamide and Furfural. *Indn. J. Engi. & Mat. Sci.* 2023; 30: 816-822.
19. Thakre M. B, Gurnule W. B. Synthesis and Characterizations of New Copolymer Resin Derived from 4-Hydroxybenzoic Acid and Adipamide. *Mat. Tod. Proc.* 2019; 15: 516-525.



20. Akare A.A, Gurnule W B, Chafle D. M. Synthesis and thermal performance of copolymer engineer for high temperature application.2025;16(6):5-18.
21. Gupta R. H, Gupta P. G, Pandit V. U, Rathod Y. U, Gurnule W. B. Non-isothermal decomposition study of copolymer derived from 2-amino 6-nitrobenzothiazole, melamine, and formaldehyde. Mat. Tod. Proc. 2021; 12: 321.
22. Gurnule W. B, Rathod Y. U, Belsare A. D, Das N. C. Thermal degradation and antibacterial study of transition metal complexes derived from novel terpolymer ligand. Mat. Tod. Proc. 2020; 29: 1044-1049.
23. Kohad C., Gurnule W. B. Synthesis, Characterization and Photoluminescence Studies of Organic Copolymer Resin. Mat. Today Proc.2019; 15: 438–446.
24. Mujafarkani N, Ahamed J. Thermal degradation investigations of newly synthesized terpolymeric polychelates. Mat. Tod. Proc. 2021; 49: 1920-1928.
25. Rathod Y. U, Pandit V. U, Bhagat D. S, Gurnule W. B. Synthesis of copolymer and its composites with carbon and their photoluminescence studies. Mat. Tod. Proc.2022; 63: 1125-1136.
26. Sidharaj N, Rajaran G, Senthil M. Synthesis, characterization and applications: Novel terpolymer and its composite. 2020; 42: 1030-1036.
27. Akare A. A, Chafle D. M, Gurnule W. B, Sethi B. Synthesis and Characterization of Copolymer Derived from 8-Hydroxyquinoline 5-Sulphonic acid, Acrylamide and Formaldehyde. Res. J. Phar. Bio. & Chem. Sci. 2024; 15: 43-49.
28. Gour S. N, Chafle D. M, Gurnule W. B., Synthesis and Characterization of Copolymer 2-AminothiophenolOxamide -Formaldehyde. Res. J. Phar. Bio. & Chem. Sci.15:83-87
29. Mandavgade S, Gurnule W. B., Synthesis and chelate ion exchange properties of copolymer resin: 8-hydroxyquinoline-5-sulphonic acid-catechol-formaldehyde. Mat. Tod. Proc. 2024; 60: 1814-1818.
30. Akare A.A, Gurnule W. B, Chafle D. M. Multifunctional copolymer synthesized using 8 hydroxyquinoline thermal spectroscopic and surface morphological analysis. J. of Appl.Bioana.2025;11(16s): 907-918.
31. Chakole S. P, Rathod Y. U, Pandit V. U, Gurnule W. B., Synthesis, characterization and thermal behavior of 2,2 dihydroxybiphenyl-formaldehyde-phenylenediamine copolymer. Mat. Tod. Proc. 2022; 56: 69-100.
32. Akare A. A, Gurnule W. B, Chafle D. M. Batch separation and thermal Kinetic studies of novel polymer. Adv. Engi, Sci. 2026;58(01):149-167.
33. El-shazlyR, KamalR, NassarA, AhmedN, SayedG. The behavior of some terpolymers as lubricating oil additives. Appl. Petro. Res. 2020; 10: 115.
34. Azarudeen R. S., Ahamed M. R, Gurnule W B., Kinetics of thermal decomposition and antimicrobial screening of terpolymer resins. Polym. Bulletin.2011; 67: 1553-1568.
35. Tarase M. V, Zade A. B, Gurnule W. B., Kinetics of thermal degradation studies of some new terpolymers derived from 2, 4-dihydroxypropiophenone, oxamide, and formaldehyde J. Appl. Polym. Sci.2009; 116: 619-627.
36. Akare A. A, Jaunjal P, Thakre J.N, Gurnule W. B, and Chafle D. M. thermal decomposition Kinetics of a copolymer derived from 8 hydroxyquinoline 5 sulphuric acid and formaldehyde. Int. J. Drug, Tech.2026;16(10);625-635.
37. W. B. Gurnule and Y. U. Rathod, Synthesis, Characterization and Thermal Behaviour Studies of Terpolymer Resin Derived from 8-Hydroxyquinoline-5-Sulphonic Acid and Anthranilic Acid, Current Appl. Polym. Sci., 2021, 4, 47-54.
38. Gurnule W. B, Rathod Y. U, Belsare A D, Das N. C. Thermal degradation and antibacterial study of transition metal complexes derived from novel terpolymer ligand. Mat. Tod. Proc. 2020; 29: 1044-1049.
39. Gurnule W. B, Butoliya S.S. Isoconversional and thermal methods of kinetic analysis of 2, 4-dihydroxybenzophenone copolymer resin. J. Appl. Polym. Sci. 2011; 122: 2181-2188.



40. Gurnule W. B, Rathod Y. U. Synthesis, Characterization and Thermal Behaviour Studies of Terpolymer Resin Derived from 8-Hydroxyquinoline-5-Sulphonic Acid and Anthranilic Acid. *Curr. Appl. Polym. Sci.* 2021; 4: 47-57.
41. Fernandes M.C.S., Branco R., Pereira P., Coelho J.F.J., Morais P.V., Serra A.C. Antimicrobial activity of copolymer structures from bio-based monomers. 2024;25(12):7915–7925.
42. Laysandra L., Rusli R.A., Chen Y.W., Chen S.J., Yeh Y.W., Tsai T.L., Huang J.H., Chuang K.S., Njotoprajitno A., Chiu Y.C. Elastic and self-healing copolymer coatings with antimicrobial function. 2024;16(19):25194–25209.
43. Konoeda Y., Tsuji T. Enhancing antibacterial activity of cationic polystyrene via copolymerization with acrylate monomers. 2025;57(5):553–565.
44. W. B. Gurnule, Jyotsna V. Khobragade, Thermal Degradation Studies Of Copolymer Resin-Iii Derived From 8-Hydroxyquinoline 5-Sulphonic Acid-Thiosemicarbazide-Formaldehyde, *J. Curr. Engg. and Scient. Res.* 2019, 6(1), 116-122

